De Novo Shoot Regeneration Controlled by HEN1 and TCP3/4 in Arabidopsis

Woorim Yang[1], Myung-Hwan Choi[1], Bosl Noh[2,*] and Yoo-Sun Noh[1,3,*]

[1]School of Biological Sciences, Seoul National University, 1 Gwanak-ro, Gwanak-gu, Seoul 08826, Korea
[2]Research Institute of Basic Sciences, Seoul National University, 1 Gwanak-ro, Gwanak-gu, Seoul 08826, Korea
[3]Plant Genomics and Breeding Institute, Seoul National University, Seoul 08826, Korea

*Corresponding authors: Yoo-Sun Noh, E-mail, ysnoh@snu.ac.kr; Fax, +82-2-871-6673; Bosl Noh, E-mail: bnoh2003@gmail.com; Fax, +82-2-871-6673.

Plants have the ability to regenerate whole plant body parts, including shoots and roots, in vitro from callus derived from a variety of tissues. However, the underlying mechanisms for this de novo organogenesis, which is based on the totipotency of callus cells, are poorly understood. Here, we report that a microRNA (miRNA)-mediated posttranscriptional regulation plays an important role in de novo shoot regeneration. We found that mutations in *HUA ENHANCER 1* (*HEN1*), a gene encoding a small RNA methyltransferase, cause cytokinin-related defects in de novo shoot regeneration. A *hen1* mutation caused a large reduction in the miRNA319 (miR319) level and a subsequent increase in its known target (*TCP3* and *TCP4*) transcript levels. TCP transcription factors redundantly inhibited shoot regeneration and directly activated the expression of a negative regulator of cytokinin response *ARABIDOPSIS THALIANA RESPONSE REGULATOR 16* (*ARR16*). A *tcp4* mutation at least partly rescued the shoot-regeneration defect and derepression of *ARR16* in *hen1*. These findings demonstrate that the miR319-TCP3/4-ARR16 axis controls de novo shoot regeneration by modulating cytokinin responses.

Keywords: ARR ● De novo shoot regeneration ● HEN1 ● miR319 ● TCP.

Accession number

Data for RNA-seq analyses have been deposited into NCBI SRA database (**https://www.ncbi.nlm.nih.gov/sra/**) and are accessible through accession number [PRJNA580054].

Introduction

Fully differentiated plant tissues can be reverted to undifferentiated states and further redifferentiated into different types of tissues by simple modulation of the ratio of auxin and cytokinin (Skoog and Miller 1957). On auxin-rich callus-induction media (CIM), divisions of pericycle or pericycle-like cells within explants lead to the formation of a regeneration capacity possessing cell mass referred to as callus (Atta et al. 2009, Sugimoto et al. 2010). Organs can be regenerated from regeneration-competent cells within callus, and their cellular and developmental fates are determined by the balance between auxin and cytokinin: shoots or roots are regenerated from callus on cytokinin-rich shoot-induction media (SIM) or auxin-rich root-induction media (RIM), respectively.

Due to the advance in genome-wide gene expression analyses and the development of various cell-type-specific reporters, the molecular genetic basis of de novo shoot regeneration has begun to be revealed in the model plant, *Arabidopsis thaliana*. At the onset of callus formation from various tissues, genes that are known to be expressed in root meristems or lateral root primordia, such as *SCARECROW* (*SCR*), *SHORT-ROOT* (*SHR*), *WUSHEL-RELATED HOMEOBOX 5* (*WOX5*) and *PLETHORAs* (*PLTs*), are highly induced (Atta et al. 2009, Sugimoto et al. 2010, Kareem et al. 2015, Kim et al. 2018). The resemblance in gene expression profiles and cellular origin between callus and the lateral root primordia suggests that callus formation from mature tissues could be a process of 'transdifferentiation' rather than 'undifferentiation' (Sugimoto et al. 2011). Recent studies have shown that some root-meristem genes are essential for the establishment and maintenance of the regenerative competence of callus (Kareem et al. 2015, Kim et al. 2018), although the underlying mechanisms of their functions are yet to be elucidated. Upon shoot induction on SIM, a number of genes that function in the establishment of the shoot apical meristem (SAM), such as *WUSHEL* (*WUS*), *CLAVATA 3* (*CLV3*) and *SHOOT-MERISTEMLESS* (*STM*), are induced and form localized and organized spatial expression patterns in the dome-shaped regions of callus similarly to the case of the SAM (Cary et al. 2002, Gordon et al. 2007). Thus, de novo shoot regeneration from callus proceeds with cell organization to establish the SAM.

MicroRNAs (miRNAs) play regulatory roles in various aspects of plant growth and development, abiotic stresses and immunity, etc., by affecting gene expression at the posttranscriptional or translational level (Sunkar et al. 2012, Li and Zhang 2016). A recent study reported the involvement of miRNAs in callus formation and de novo shoot regeneration (Qiao and Xiang 2013). Furthermore, miRNA160 (miR160) was reported to prevent callus formation by reducing the expression of its target *AUXIN RESPONSE FACTOR 10* (*ARF10*), which represses *ARABIDOPSIS THALIANA RESPONSE REGULATOR 15* (*ARR15*), a negative regulator of cytokinin response (Liu et al. 2016). Decreased levels of

miR156, a regulator of the juvenile-to-adult phase transition, and subsequently increased expressions of its targets, *SQUAMOSA PROMOTER BINDING PROTEIN-LIKE* (*SPLs*), were shown to be responsible for the reduced regeneration capacity of old plants as SPL proteins prevent the function of the type-B ARRs, which are positive regulators of cytokinin response (Zhang et al. 2015). In addition, it was reported that the ARGONAUT 10 (AGO10)-mediated repression of miR165/166 represses in vitro shoot regeneration (Xue et al. 2017). However, only a few miRNAs and their targets that are involved in the regulation of de novo shoot regeneration have been identified in these days. Furthermore, deep understandings of specific miRNA-regulatory modules involved in de novo organogenesis are currently very limited.

The miRNA319 (miR319)-TCP (TEOSINTE BRANCHED 1, CYCLOIDEA and PROLIFERATING CELL NUCLEAR ANTIGEN BINDING FACTOR) pathway has been reported to control cell division and differentiation during leaf development (Efroni et al. 2008, Koyama et al. 2017). TCPs are plant-specific transcription factors, and *TCP2/3/4/10/24* of the 24 *TCP*-family genes contains target sites for miR319. Double or triple knockouts for the miR319-regulated *TCP* genes show crinkled leaves, whereas single knockouts present slight effects on leaf morphology (Schommer et al. 2008, Koyama et al. 2010). In the miR396-GRF (GROWTH-REGULATING FACTOR) pathway, which has been reported to be downstream of the miR319-TCP pathway, miR396 plays roles in leaf growth and development by repressing *GRF* expression (Liu et al. 2009, Rodriguez et al. 2010). *AtGRF1* and *AtGRF3* were suggested to regulate cell proliferation during root and leaf development (Kim and Kende 2004, Hewezi et al. 2012).

In this study, we show that HUA ENHANCER 1 (HEN1), a small RNA 2′-*O*-methyltransferase stabilizing target miRNAs and small-interfering RNAs, modulates cytokinin responses and de novo shoot-regeneration capacity. Through gene expression analyses and characterization of mutants and overexpression plants, we found that HEN1-regulated miR319 and its targets, *TCP3* and *TCP4*, act as crucial modulators of de novo shoot organogenesis by regulating *ARR16*, a negative regulator of cytokinin response. Thus, our study demonstrates that HEN1 promotes de novo shoot regeneration from callus mainly via the miR319-TCP-ARR16 axis and illuminates an miRNA-mediated cytokinin signaling pathway that plays an important role in de novo shoot regeneration.

Results

Mutations in *HEN1* result in defective de novo shoot regeneration

We previously reported global changes in gene expression during callus development and de novo shoot organogenesis (Kim et al. 2018). As a part of our efforts to understand the roles of epigenetic and posttranscriptional gene regulation in de novo organogenesis, we studied the callus-forming and organ-regenerating abilities of *HEN1* mutants, namely *hen1-5* (Vazquez et al. 2004), *hen1-6* (Earley et al. 2010) and *hen1-10*. *hen1-10* is a new mutant allele of *HEN1* identified from our

mutant population carrying one base-pair deletion in the fifth exon of *HEN1* that leads to an early stop codon at amino acid 641 (**Fig. 1A**). *hen1-10* showed the same developmental defects, such as clustered influorescence and size-reduced and abnormally shaped leaves, as have been reported in other *hen1* mutant alleles (Vazquez et al. 2004, Earley et al. 2010) (**Supplementary Fig. S1A**). Along with the point mutation leading to an early stop codon, the *HEN1* transcript level was also reduced in the *hen1-10* (**Supplementary Fig. S1B**).

On CIM, callus formation and proliferation of all *hen1* mutant alleles tested seemed normal (**Fig. 1B**). When calli were transferred onto RIM or SIM, although the root regeneration of the mutants seemed equal to the wild-type (WT) Columbia (Col) (**Fig. 1C**), shoot regeneration was largely compromised compared to WT in all mutant alleles tested (**Fig. 1D**). Thus, *HEN1* is required for de novo shoot regeneration but not for callus formation or root regeneration.

Mutations in *hen1* decrease cytokinin responses

As cytokinin is a key signaling component in de novo shoot regeneration, we questioned whether the shoot-regeneration defect of *hen1* is related to cytokinin response. In the absence of auxin (indole-3-acetic acid; IAA), a low dosage (150 μg/l) of cytokinin (N^6-2-isopentenyl adenine; 2IP) caused pre-CIM-incubated WT but not *hen1* root explants to regenerate shoots (**Fig. 1E**). We then tested if elevated levels of cytokinin with fixed auxin dosage (150 μg/l of IAA) can rescue the shoot-regeneration defect of *hen1*. As expected, shoot regeneration in WT was more prominent with increased cytokinin dosage (**Fig. 1E**). Notably, shoot formation in *hen1* mutants was more clearly observed with 5,000 μg/l of cytokinin, which is 5.6 times the amount in regular SIM (**Fig. 1E, F**), suggesting that reduced cytokinin responsiveness could be a reason for the shoot-regeneration defect of *hen1*. Consistent with the above, we found that in planta cytokinin responses are also impaired in *hen1* mutants. A total of 5 μM of 6-benzyladenine (BA) treatment in WT seedlings caused approximately 2.5-fold increase in anthocyanin levels and approximately 36% decrease in root elongation, whereas the increase in anthocyanin levels was <2-fold and the decrease in root elongation was not obvious in *hen1-10* seedlings (**Supplementary Fig. S1C**, D).

Then, we monitored cytokinin signaling during SIM incubation using TCS (*Two-Component Signaling sensor*)::*GFP*, which reflects the transcription activity of the type-B response regulators, positive transcription activators in cytokinin signaling cascade (Iwase et al. 2011, Meng et al. 2017). *TCS::GFP* fluorescence of similar pattern and strength was detected in WT and *hen1-10* calli incubated on SIM for 3 d (**Fig. 1G**). However, after 6 or 12 d of SIM incubation, the number of cells expressing *TCS::GFP* was greatly increased in WT but clearly with less extent in *hen1-10*. Therefore, the *hen1-10* mutation appears not to disturb the initial transcriptional response of cytokinin but rather the later propagation or amplification of it during SIM incubation. We also monitored auxin response during shoot regeneration using the *DR5::GUS* reporter system. The *DR5*-promoter activity shown as GUS expression was detected in the entire root explants during early CIM incubation, and then, auxin
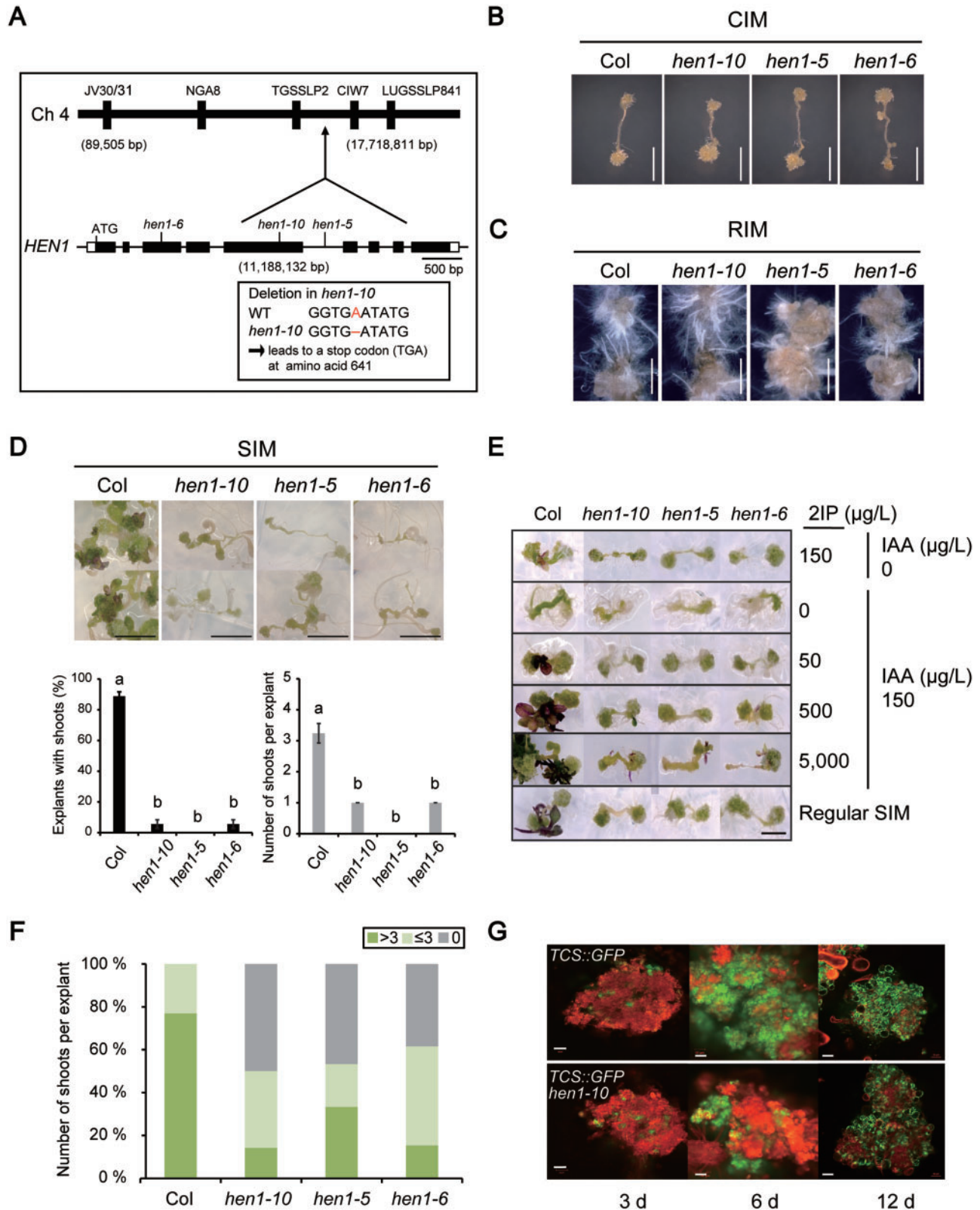
Fig. 1 De novo shoot regeneration is impaired in *hen1* mutants. (A) Identification of the *hen1-10* allele. The *hen1-10* allele was identified through map-based cloning and whole-genome sequencing and finally shown to have a single-base deletion that results in an early stop codon at the amino acid 641 of the HEN1-coding sequence. (B) Callus formation in Col (WT), *hen1-5*, *hen1-6* and *hen1-10* explants. Root explants of each genotype were transferred onto CIM for 2 weeks. Scale bars: 0.1 cm. (C) Root regeneration in Col, *hen1-5*, *hen1-6* and *hen1-10* explants. Root explants of each genotype were first incubated on CIM for 2 weeks and then transferred onto and further incubated on RIM for 2 weeks. Scale bars: 0.5 cm. (D) Shoot regeneration in Col, *hen1-5*, *hen1-6* and *hen1-10* explants. Root explants of each genotype preincubated on CIM for 1 week were transferred onto and

maxima were gradually established in specified callus masses (**Supplementary Fig. S1E**). After moving onto SIM, which has lower auxin concentration than CIM, the GUS activity decreased substantially especially after prolonged SIM incubation both in WT and *hen1-10* (**Supplementary Fig. S1E**). Thus, unlike cytokinin response, the auxin response of *hen1-10* seemed similar to that of WT on both CIM and SIM, suggesting that *HEN1* might not have a heavy role in auxin response during de novo shoot regeneration.

Identification of candidate genes responsible for the shoot-regeneration defect of *hen1*

To identify molecular components responsible for the shoot-regeneration defect of *hen1*, we then obtained and compared transcriptomes expressed during the shoot-regeneration process of WT and *hen1-10* by RNA-seq. The overall numbers of differentially expressed genes (DEGs) during the transition from roots to calli (R vs C) and from calli to shoot progenitor-containing calli (C vs S) were comparable between WT and *hen1-10* (**Fig. 2A, B**). DEG analyses between WT and *hen1-10* showed that more or less than 1,000 genes were downregulated or upregulated in *hen1-10* compared to WT in all tissues examined (**Fig. 2C** and **Supplementary Data**set S1). The largest number of DEGs was found in the upregulated S (**Fig. 2C**), suggesting that the shoot-regeneration process might be most significantly affected by the mutation in *HEN1* consistent with the shoot-regeneration defects of *hen1* mutants (**Fig. 1D**). Genes that have recently been reported to be required for the acquisition of pluripotency in callus, such as *CUP-SHAPED COTYLEDON 2* (*CUC2*), *PLTs*, *SCR* and *WOXs* (**Kareem et al. 2015, Kim et al. 2018**), were not found as DEGs between WT and *hen1-10* (**Supplementary Table S1**), and reverse-transcribed (RT)-quantitative PCR (qPCR) analyses also confirmed that the transcript levels of *SCR*, *WOX5* and *CUC2* in R, C and S were not significantly affected by the *hen1-10* mutation (**Supplementary Fig. S2A**). Calli are known to derive from dividing cells in the xylem-pole pericycle (**Atta et al. 2009**), and consistent with the normal callus-formation phenotypes of *hen1* mutants (**Fig. 1B**), expression of the pericycle marker *J0121* (**Laplaze et al. 2007**) was comparable between WT and *hen1-10* throughout CIM- and SIM-incubation periods (**Supplementary Fig. S2B**).

Because the loss of *HEN1* results in the reduction of most functional miRNAs (**Park et al. 2002**), by employing the list of predicted miRNA targets (**Bülow et al. 2012**), we then searched for potential miRNA-target genes among the DEGs that were upregulated [Trimmed Means of M values (TMM) ratio ≥ 2] in

S but not downregulated (TMM ratio > 0.5) in R and C by the *hen1-10* mutation. Based on these criteria, 145 genes were identified as the candidate targets of HEN1-modified miRNAs in S (**Supplementary Table S2**). It has been reported that miR160 promotes shoot regeneration (**Qiao et al. 2012**) as well as callus initiation via its target *ARF10* which represses the expression of *ARR15*, a negative regulator of cytokinin signaling (**Liu et al. 2016**). Considering the normal callus-formation phenotype of *hen1* mutants (**Fig. 1B**) and no significant changes in *ARR15* expression in *hen1-10* (**Supplementary Data**set S1), *ARF10* and other miR160-target *ARFs*, such as *ARF16* and *ARF17*, were not further investigated.

On the other hand, several groups of genes that are known to be miRNA targets and involved in leaf development and differentiation displayed misregulation by the *hen1-10* mutation (**Table 1** and Supplementary S2). These included *TCP3/4* (**Schommer et al. 2008, Koyama et al. 2010**), *GRF1/4/9* (**Liu et al. 2009, Rodriguez et al. 2010**) and *SPL3/6* (**Zhang et al. 2015**). Therefore, we tested whether the misregulations of these genes are responsible for the shoot-regeneration defect of *hen1* as described in the following sections.

MiR156-targeted *SPLs* are unlikely responsible for the shoot-regeneration defect of *hen1*

Among miR156-targeted *SPLs*, the *SPL9*-group genes (*SPL2/6/9/10/11/13/15*) but not the structurally distinct *SPL3*-group genes were shown to cause a progressive decline in shoot-regeneration capacity by inhibiting the function of the type-B *ARRs* (**Zhang et al. 2015**). We reexamined the expressions of *SPL2/3/6/9/10/15* in WT vs *hen1* by RT-qPCR and found that their transcript levels were clearly and significantly increased by *hen1-10* in R but not or less significantly in C and S (**Supplementary Fig. S3A**). When miR156-resistant forms of *SPL3* (*35S:rSPL3*) and *SPL9* (*pSPL9:rSPL9*) were expressed, although the number of shoots formed per explant was decreased significantly, the percentage of explants with shoots formed was not significantly reduced in both cases (**Supplementary Fig. S3B**, C). Considering the large reductions in the all shoot-regeneration scorings of *hen1* mutants (**Fig. 1D**), the results above implied that the misregulation of *SPL3* and *SPL6* is not likely a major reason for the shoot-regeneration defect of *hen1*.

MiR396-targeted *GRFs* are unlikely responsible for the shoot-regeneration defect of *hen1*

MiR396-target *GRFs* (*GRF1/2/3/4/7/8/9*) have been shown to be involved in leaf and other organ development by positively regulating cell proliferation (**Horiguchi et al. 2005**, **Gonzalez**

Fig. 1 Continued
further incubated on SIM for 4 weeks before scoring for explants with shoots (%) and the number of shoots per explant. Scale bars: 0.5 cm. Shown are the means ± SE of three biological replicates (*n* = 12 explants of each genotype per replicate). Different letters indicate significant differences between genotypes according to one-way ANOVA with Tukey's post hoc test (*P* < 0.05). (E) Shoot-regeneration assay using Col, *hen1-5*, *hen1-6* and *hen1-10* explants on media with different cytokinin-to-auxin ratios. Root explants of each genotype were preincubated on CIM for 2 weeks and then transferred onto and incubated for 3 weeks on SIM containing indicated amounts of IAA and 2IP. The regular SIM contained 158 μg/l of IAA and 894 μg/l of 2IP. Scale bar: 0.5 cm. (F) Number of shoots per explant on SIM containing 150 μg/l of IAA and 5,000 μg/l of 2IP. Shoots were scored at 3 weeks on SIM after 2 weeks of CIM incubation of root explants (*n* ≥ 13 per genotype). (G) *TCS::GFP* signals in the root explants of WT and *hen1-10*. Root explants of each genotype preincubated on CIM for 2 weeks were transferred onto and further incubated on SIM for indicated days before confocal imaging. Cellular outlines were visualized with PI staining (red). Scale bars: 50 μm.
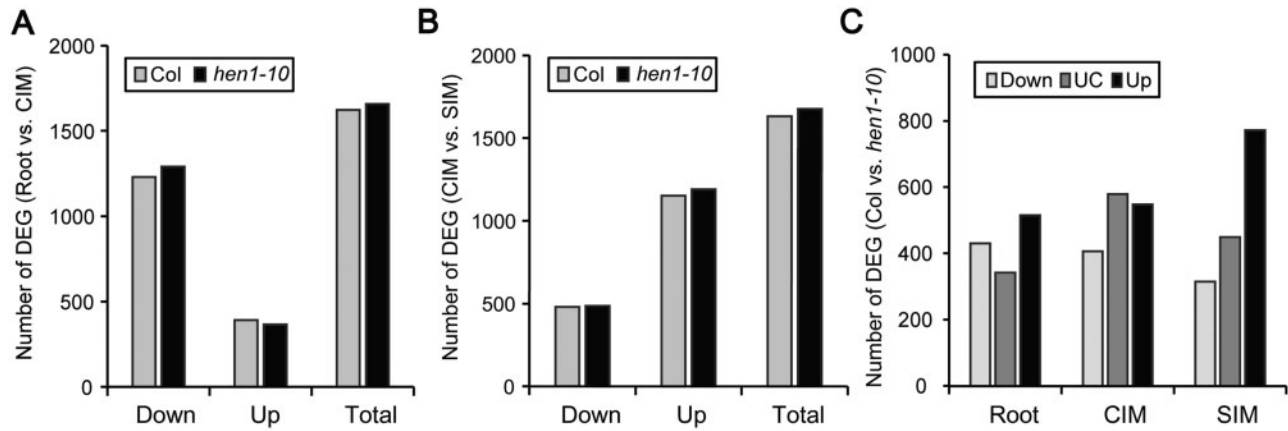
Fig. 2 Mutation in *HEN1* primarily affects genes upregulated in SIM. (A and B) Statistic chart of DEGs between roots and CIM-incubated root explant (A) or between CIM-incubated root explants and CIM-incubated + SIM-incubated root explants (B) of Col and *hen1-10*. (C) DEGs between Col and *hen1-10* roots, CIM and SIM. DEGs were identified from RNA-seq data obtained using roots of 2-week-old seedlings, CIM and SIM. CIM: root explants after 7-day incubation on CIM; SIM: root explants after 7-day incubation on CIM followed by 4-day incubation on SIM. ≥2-Fold downregulated or upregulated genes with EdgeR *P*-value <0.05 are shown. UC: unchanged (<2-fold changed) genes.

Table 1 Potential miRNA-target genes upregulated in *hen1-10* on SIM and implicated in leaf differentiation and development

Gene ID	Gene name	miRNA [a]		Root			CIM			SIM		
				Col	hen1-10	FC	Col	hen1-10	FC	Col	hen1-10	FC
AT1G69170	SPL6	miR156	Wang et al. (2018)	502.47	708.09	1.41	268.07	418.52	1.56	177.66	364.61	2.05
AT2G33810	SPL3			0.00	37.66		0.00	0.00		0.00	8.41	
AT2G32460	MYB101	miR159	Tang et al. (2012) and	3.53	2.12	0.60	10.49	12.96	1.24	12.90	38.33	2.97
AT3G11440	MYB65		Wang et al. (2018)	220.05	838.27	3.81	232.78	765.74	3.29	169.72	563.74	3.32
AT5G06100	MYB33			648.39	1,462.75	2.26	891.03	1,725.93	1.94	580.63	1,224.70	2.11
AT1G48410	AGO1	miR168	Vazquez et al. (2004)	10,328.30	18,255.74	1.77	9,894.87	22,169.43	2.24	7,987.85	17,023.35	2.13
AT1G53230	TCP3	miR319	Tang et al. (2012), Ren et al. (2014)	115.32	415.96	3.61	68.69	225.00	3.28	116.13	476.79	4.11
AT3G15030	TCP4		and Tsai et al. (2014)	137.68	656.22	4.77	238.50	799.07	3.35	208.43	726.41	3.49
AT2G22840	AtGRF1	miR396	Zhao et al. (2012)	941.40	1,416.17	1.50	276.66	400.93	1.45	330.51	670.31	2.03
AT2G45480	AtGRF9			96.49	95.26	0.99	8.59	9.26	1.08	13.90	31.79	2.29
AT3G52910	AtGRF4			345.96	382.09	1.10	19.08	23.15	1.21	62.53	131.82	2.11
AT5G05390	LAC12	miR408	Unknown	195.34	111.13	0.57	157.41	195.37	1.24	112.16	232.79	2.08
AT3G09220	LAC7	miR857	Unknown	8,126.60	7,116.86	0.88	274.75	253.70	0.92	212.40	462.77	2.18
AT5G14340	MYB40	miR858	Zhao et al. (2012)	22.36	21.17	0.95	0.00	0.00		29.78	99.10	3.33

Shown are trimmed RPKM values from the RNA-seq data obtained from the roots, CIM and SIM. Roots: roots of 2-week-old seedlings; CIM: root explants after 7-day incubation on CIM; SIM: root explants after 7-day incubation on CIM followed by 4-day incubation on SIM.

FC: fold change.

[a]References for the involvement of HEN1 in stabilizing corresponding miRNAs.

et al. 2010). *GRF1, GRF2, GRF4* and *GRF9* were identified as upregulated DEGs from our RNA-seq analysis (**Supplementary Table S2**), and the increased *GRF1* transcript levels in *hen1-10* were also confirmed by RT-qPCR analysis (**Supplementary Fig. S4A**). Therefore, we examined if the upregulation of *GRF1* is related to the shoot-regeneration defect of *hen1* by assessing the shoot-regeneration phenotype of plants overexpressing an miR396-resistant form of *GRF1* (*35S::rGRF1*; Hewezi et al. 2012; **Supplementary Fig. S4B**). Consistent with the role of *GRFs* in cell proliferation, *35S::rGRF1* calli grew faster than WT calli (**Supplementary Fig. S4C**). However, the shoot-regeneration efficiency of *35S::rGRF1* was not distinguishable from that of WT (**Supplementary Fig. S4D, E**), pointing to

the fact that the upregulation of *GRF1* or other *GRF*-family members might not be a major reason for the shoot-regeneration defect of *hen1*.

MiR319-targeted *TCPs* repress shoot regeneration

MiR319-targeted *TCPs* (*TCP2/3/4/10/24*) encode well-known transcription factors that regulate multiple aspects of development, especially leaf development (Palatnik et al. 2003, Efroni et al. 2008). Because a few previous studies have reported an additional role of TCPs in shoot-meristem function (Koyama et al. 2007, Efroni et al. 2008), we studied if the upregulated *TCP3/4* is responsible for the shoot-regeneration defect of *hen1*. First, we examined the expression levels of miR319 and

miR319-targeted *TCPs* by RT-qPCR analysis. Mature miR319 levels were substantially decreased in *hen1-10* throughout the de novo shoot-regeneration process (**Fig. 3A**). Conversely, in agreement with the RNA-seq result (**Table 1** and Supplementary S2), the transcript levels of *TCP3/4* but not *TCP2/10/24* were significantly increased in *hen 1-10* compared to WT (**Fig. 3B** and **Supplementary Fig. S5A**). When the role of TCPs in de novo shoot regeneration was investigated by using transgenic plants expressing an miR319-resistant form of *TCP4* (*rTCP4-GFP*; **Supplementary Fig. S5B**), the number of explants with shoots formed and the number of shoots per explant were substantially reduced in *rTCP4-GFP* lines (**Fig. 3C–E**). Consistently, the overexpression of an miR319-resistant form of *TCP3* (*35S::mTCP3*; Koyama et al. 2007) also resulted in significant reductions in shoot regeneration (**Fig. 4A–C**). By contrast, a triple mutant for the miR319-target *TCP3/4/10* (Schommer et al. 2008, Koyama et al. 2010) displayed greatly enhanced shoot-regeneration efficiencies compared to WT (**Fig. 4A–C**). The addition of mutations in *TCP5* and *TCP13*, which are not miR319 targets, to *tcp3/4/10* (*tcp3/4/5/10/13*; Schommer et al. 2008, Koyama et al. 2010) slightly boosted the shoot-regeneration phenotypes of *tcp3/4/10* (**Fig. 4A–C**), indicating that the TCPs are strong negative regulators of de novo shoot regeneration. Among WT explants, the CIM-incubation period was more critical in determining regenerative capacity than the following SIM-incubation period: explants with long CIM-incubation periods exhibited a higher number of regenerated shoots compared to explants with short CIM-incubation periods (**Figs. 1D, 3E, 4B**). Hence, we set the CIM-incubation period to 1 week this time to assess the effects of *tcp* mutations on enhanced shoot regeneration (**Fig. 4A–C**).

Therefore, the results above suggested that the substantial upregulation of *TCP3* and *TCP4* by the reduction in miR319 might be a major reason for the shoot-regeneration defect of *hen1*. To further verify this possibility, we generated a double mutant between *hen 1–6* and *tcp4-1* (Schommer et al. 2014) and examined its shoot-regeneration phenotype. Remarkably, the shoot-regeneration defect of *hen1-6* was significantly rescued by the *tcp4-1* single mutation; the number of explants with shoots formed was recovered to WT level and the number of shoots per explant was also increased to the 53% level of WT (**Fig. 5A–C**). The transcript level of *TCP3* in *hen1-6* was unchanged by the *tcp4-1* mutation (**Fig. 5D**), suggesting that the increased expression of *TCP3* might be a reason for the incomplete rescue of the number of shoots per explant in *hen1-6 tcp4-1*. Taken together, these data point to the fact that the miR319-TCP3/4 module is required for legitimate de novo shoot regeneration.

TCP4 directly activates *ARR16* during de novo shoot regeneration

Then, we questioned how the miR319-TCP module regulates de novo shoot regeneration. TCPs were previously proposed to negatively regulate the organ-boundary *CUC* genes by

activating miR164 transcription during lateral-organ and shoot-meristem development (Koyama et al. 2010). However, our RNA-seq data and RT-qPCR analyses showed no significant reduction in *CUC1* and *CUC2* expression by the *hen1-10* mutation in S (**Supplementary Table S1** and Figs. S2B, S6A, C). In line with this, the *pri-miR164* transcript level was also comparable between WT and *hen1-6* in S (**Supplementary Fig. S6B**).

A previously reported interesting role of miR319-targeted *TCPs* is to decrease the cytokinin sensitivity in leaves by directly activating the transcription of *ARR16* and *ARR6*, negative regulators of cytokinin response (Efroni et al. 2013). In addition, several type-A ARRs, such as ARR16, were reported to negatively control the shoot-regeneration capacity of hypocotyl explants (Ren et al. 2009). Furthermore, multiple mutants for type-A *ARRs* showed enhanced de novo shoot-regeneration phenotypes (Buechel et al. 2010).

Hence, we first examined *ARR16* expression in WT and *hen1* throughout the de novo shoot-regeneration process. *ARR16* expression was greatly induced on SIM in WT, and this induction was further enhanced by the *hen1-10* mutation (**Fig. 6A, B** and **Supplementary Table S3**), whereas the expressions of other type-A *ARRs*, including *ARR6*, were not substantially different between WT and the mutant throughout the regeneration process (**Supplementary Table S3**). However, the expression of *ARR16* on SIM was greatly reduced by the *tcp4-1* mutation both in WT and *hen1-10* (**Fig. 6B**). On the other hand, the expression of *ARR16* and other previously known TCP4 targets, such as *LIPOXYGENASE 2* (*LOX2*) and *pri-miR396* (Efroni et al. 2013), was significantly increased by *rTCP4-GFP* on SIM (**Fig. 6C**). Therefore, these results indicate that the previously reported TCP4-dependent activation of *ARR16* in leaves is also observed during de novo shoot regeneration from callus. Furthermore, our chromatin immunoprecipitation (ChIP) assays using SIM-incubated explants showed the direct targeting of TCP4-GFP to the *ARR16*-promoter region containing TCP4-binding motifs (Efroni et al. 2013) as well as to the promoters of *LOX2* and *MIR396* (**Fig. 6D, E**). Thus, together with the cytokinin-hyposensitive phenotypes of *hen1* in callus and seedling (**Fig. 1E–G** and **Supplementary Fig. S1C**, D), the results above indicate that the HEN1-miR319-TCP3/4-ARR16 axis modulates cytokinin responses on SIM and constitutes a regulatory module for de novo shoot regeneration. The lower level of *ARR16* expression in *hen1-6 tcp4-1* than in WT (**Fig. 6B**) yet the incompletely restored shoot-regeneration phenotype of *hen1-6 tcp4-1* (**Fig. 5C**) suggests that HEN1 might also affect de novo shoot regeneration via factor(s) other than the miR319-TCP-ARR16 module.

The *WUS* expression pattern is altered in *hen1*

Cytokinin defines and maintains the stem-cell niche in the SAM by regulating *WUS* (Xie et al. 2018). Because *WUS* is also required for shoot-meristem formation during de novo shoot organogenesis (Gordon et al. 2007, Chatfield et al. 2013, Zhang et al. 2017), we studied if the shoot-regeneration defect of *hen1* is related with *WUS* expression using *pWUS::mGFP5-ER* (**Fig. 7A**). In WT, GFP fluorescence was not detected at 3 d on SIM, begun to be visible as scattered spots at 6 d and,

A

B

C

D

E
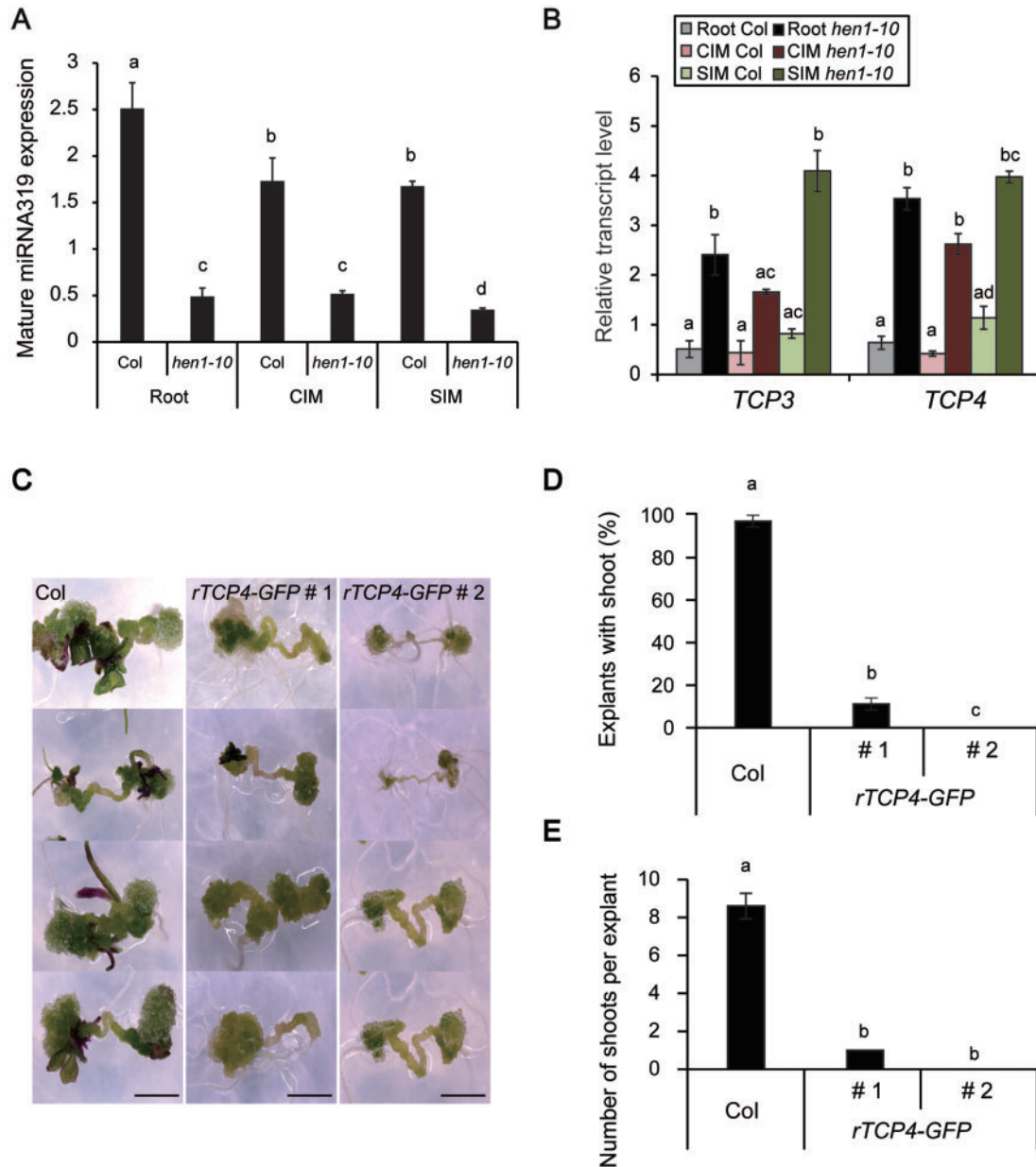
Fig. 3 miR319-regulated *TCP4* is involved in de novo shoot regeneration. (A) Expression of mature miR319 in Col and *hen1-10* as determined by stem-loop RT-qPCR. The small nuclear RNA U6 was used as an expression control for normalization. Shown are the means ± SE of three biological replicates. (B) The transcript levels of *TCP3* and *TCP4* in Col and *hen1-10*. Ubiquitin 10 (*UBQ10*) was used as an expression control for normalization. Roots of 2-week-old seedlings, 7 d CIM-incubated root explants and 7 d CIM-incubated + 4 d SIM-incubated root explants were used for RNA extraction (A and B). Shown are the means ± SE of three biological replicates. (C) Shoot-regeneration defect of *pTCP4::rTCP4:GFP* (*rTCP4-GFP*) transgenic plants. Two weeks CIM-incubated root explants were transferred onto and further incubated on SIM for 2 weeks before picturing. Two independent T3 transgenic lines of *rTCP4-GFP* (# 1 and # 2) were used for the shoot-regeneration assay. Photographs of four representative explants per genotype are shown. Scale bars: 0.5 cm. (D) Explants with shoot in Col and *pTCP4::rTCP4:GFP* (*rTCP4-GFP*) transgenic plants as scored at 2 weeks on SIM after 2 weeks of CIM incubation of root explants. Shown are the means ± SE of three biological replicates ($n = 20$–36 explants of each genotype per replicate). (E) Number of shoots per explant as scored at 2 weeks on SIM after 2 weeks of CIM incubation of root explants. Shown are the means ± SE ($n = 83$ for Col, 112 for lines # 1 and 84 for line # 2). Statistical analysis of data was performed by one-way ANOVA with Tukey's post hoc test. Different letters represent significantly different groups ($P < 0.05$) (A, B, D, E).

then, formed discrete domains (presumably marking shoot apical-meristem progenitors) at 12 d. However, in *hen1-6*, GFP fluorescence was not detected until 6 d on SIM and, then, detected as scattered spots instead of forming discrete domains at 12 d. *WUS* transcript level was also reduced in *hen1-6*

compared to WT at 12 d on SIM (**Fig. 7B**). Therefore, the hyper-activated miR319-TCP3/4-ARR16 module in *hen1* might induce decreased cytokinin sensitivity, and which, in turn, may result in the failure of proper temporal and spatial *WUS* expression, finally leading to the defective de novo shoot organogenesis.
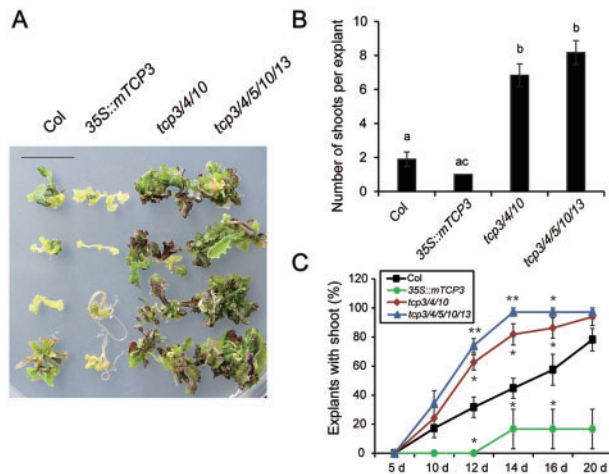
Fig. 4 Functionally redundant TCP transcription factors negatively affect shoot regeneration. (A) Shoot regeneration in Col, *35S::mTCP3*, *tcp3/4/10* and *tcp3/4/5/10/13*. One-week CIM-incubated root explants were transferred onto and further incubated on SIM for 20 d before picturing. Photographs of four representative explants per genotype are shown. Scale bar: 1 cm. (B) Number of shoots per explant as scored at 20 d on SIM after 1 week of CIM incubation of root explants. Shown are the means ± SE ($n = 32$ for Col, 13 for *35S::mTCP3*, 40 for *tcp3/4/10* and 41 for *tcp3/4/5/10/13*). Different letters represent statistically significant different groups ($P < 0.05$) by one-way ANOVA with Tukey's post hoc test. (C) Explants with shoot in Col, *35S::mTCP3*, *tcp3/4/10* and *tcp3/4/5/10/13* as scored at indicated days on SIM. Root-derived explants were incubated on CIM for 1 week before transferring onto SIM. Shown are the means ± SE of three biological replicates ($n = 14–18$ for Col, 3–6 for *35S::mTCP3*, 11–18 for *tcp3/4/10* and 12–18 for *tcp3/4/5/10/13* per replicate). Asterisks indicate statistically significant differences from Col (*$P < 0.05$ and **$P < 0.005$ in Student's *t*-test).

Discussion

As in planta developmental processes, de novo organogenesis from plant tissues is guided by the proper balance of phytohormones especially auxin and cytokinin. Therefore, the recognized in planta roles of miRNAs in diverse aspects of plant development and various phytohormone responses suggest the roles of miRNAs also in de novo organogenesis. However, specific miRNAs engaged in de novo organogenesis and the regulatory pathways directed by them are yet to be understood. Our study using *hen1* mutants shows that the disruption of miRNA homeostasis impairs de novo shoot regeneration from Arabidopsis root explants. In detail, we identified that the miR319-TCP3/4-ARR16 as a regulatory axis in the complicated miRNA regulation of shoot regeneration (**Supplementary Fig. S7**).

De novo shoot regeneration from root explants is processed through multiple steps, including the acquisition of shoot-regeneration competence (i.e. pluripotency) on CIM, the formation of shoot progenitors on SIM and the final shoot development from shoot progenitors. No visible aberration in callus formation and no reduction in the expression of pluripotency genes, such as *WOX5*, *PLT1/2*, *SCR* and *CUC1/2*, in *hen1* calli suggest that miRNAs stabilized and matured by HEN1 might not play key regulatory roles in callus growth and pluripotency

acquisition. In line with this, unlike *hag1* mutants, which are defective of shoot regeneration due to the failure of pluripotency acquisition (Kim et al. 2018), the shoot-regeneration defect of *hen1* mutants was partially rescued by increased cytokinin-to-auxin ratios on SIM. Therefore, the roles of miRNAs appear to be more important in later shoot-developmental processes on SIM where cytokinin acts as an important modulator than in pluripotency-acquisition processes on CIM where auxin has a prominent role.

WUS, a key regulator of shoot-meristem maintenance in planta, is also essential for de novo shoot regeneration (Meng et al. 2017, Zhang et al. 2017). Notably, several recent reports have shown that *WUS* is a direct target of type-B ARRs and type-B ARR-activated *WUS* expression is an underlying mechanism for the cytokinin-mediated establishment of shoot stem-cell niche (Meng et al. 2017, Wang et al. 2017, Zubo et al. 2017). Thus, it is likely that the miR319-TCP3/4-ARR16 module also has an important role in ensuring proper *WUS* expression and sufficient *WUS*-positive cell clusters representing shoot progenitor regions (Zhang et al. 2017) during de novo shoot regeneration.

Our study provides new roles of miR319 and its target *CINCINNATA* (*CIN*)-like *TCPs* in de novo shoot regeneration. miR319 and *CIN*-like *TCPs* are well-known key players in leaf development and growth that act by controlling cell proliferation. However, the possibility of *TCP3/4* induction in *hen1* via miR319-independent mechanisms remains. The expression profiles of miR319-target *TCPs* during shoot regeneration (root–CIM–SIM) were not identical to each other nor perfectly reflected the expression profile of mature miR319 (**Fig. 3A, B** and **Supplementary Fig. S5A**). Therefore, *TCP3/4* mRNA levels could be increased in *hen1* not only via miR319 but also via other mechanisms. Alternatively, the regulation imposed on *TCP2/10/24* by other factors might be strong enough to override the effect of altered miR319 activity in *hen1*.

Thus, our study proposes that leaf growth regulators, such as TCPs, also have a role in de novo shoot organogenesis. Notably, a few earlier studies have reported shoot-meristem-related roles of *CIN*-like *TCPs*: precocious expression of miR319-resistant *TCP4* (*rTCP4*) in emerging primordia resulted in miniature cotyledons and shoot apical-meristem termination (Efroni et al. 2008), and ectopic expression of miR319-resistant *TCP3* (*35S::mTCP3*) caused the failure of shoot-meristem formation in leaf exile (Koyama et al. 2007). Therefore, questions on how TCPs regulate both leaf growth and shoot-meristem establishment or maintenance would be interesting and challenging. Regarding this, there was a recent report that might be relevant to such dual roles of TCPs: concurrent reduction of CIN-like TCPs and functionally redundant NGATHA (NGA) transcription factors caused an indeterminate growth of the leaf margin, of which growth is otherwise determinate, and continued organogenesis relying on WOXs, suggesting the existence of leaf meristems that are suppressed by CIN-like TCPs and NGAs (Alvarez et al. 2016). Notably, it was reported that *TCP3* transcripts are not detected in the shoot meristem and its boundary regions despite the strong *TCP3* promoter activity in those tissues and
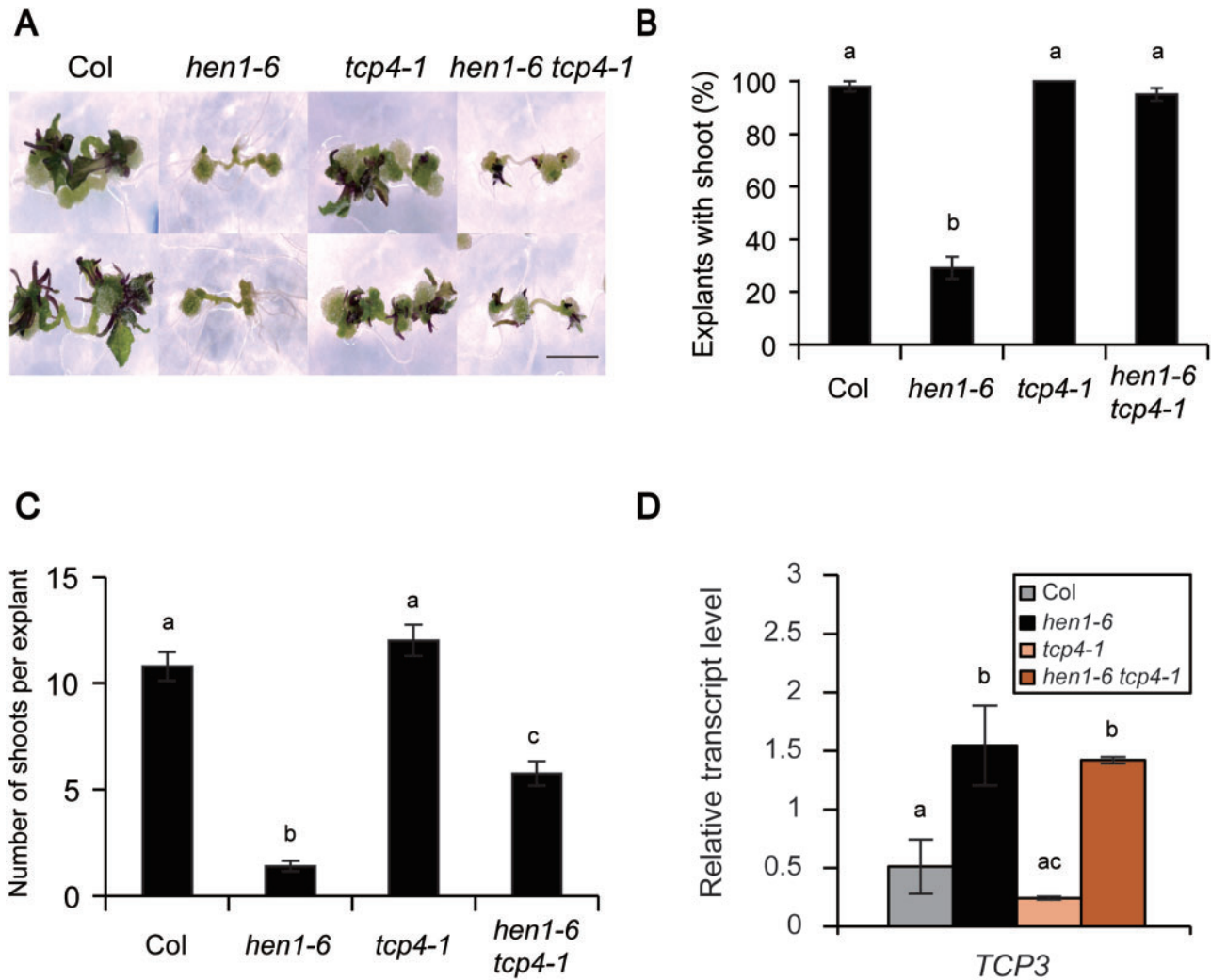
Fig. 5 The *tcp4-1* mutation partially rescues the shoot-regeneration defect of *hen1-6*. (A) Shoot regeneration in Col, *hen1-6*, *tcp4-1* and *hen1-6 tcp4-1*. Two-week CIM-incubated root explants were transferred onto and further incubated on SIM for 14 d before picturing. Photographs of two representative explants per genotype are shown. Scale bar: 0.5 cm. (B and C) Explants with shoot (B) and the number of shoots per explant (C) were scored at 2 weeks on SIM after 2 weeks of CIM incubation of root explants. Shown are the means ± SE of three biological replicates ($n \geq 42$ for Col, ≥ 5 for *hen1-6*, ≥ 42 for *tcp4-1* and ≥ 56 for *hen1-6 tcp4-1* per replicate). (D) RT-qPCR analysis of *TCP3* transcript levels in Col, *hen1-6*, *tcp4-1* and *hen1-6 tcp4-1* root-derived explants incubated 7 d on CIM + 4 d on SIM. *UBQ10* was used as an internal control for normalization. Shown are the means ± SE of three biological replicates. Different letters indicate statistically significant different groups ($P < 0.05$) by one-way ANOVA with Tukey's post hoc test (B–D).

the abortion of shoot-meristem initiation by the ectopic expression of miR319-resistant *TCP3* (Koyama et al. 2007). These results altogether suggest that miR319-targeted *CIN*-like *TCPs* might function as suppressors of meristem activity in both shoot and leaf meristems. Thus, proper spatiotemporal control of miR319-regulated TCP activity might be critical for shoot-meristem formation and organ development both in planta and in de novo organogenesis.

The role of TCPs in leaf development is known to be exerted mostly by repressing the expression of *CUC1* and *CUC2* by activating *MIR164* transcription (Koyama et al. 2010). The TCP-miR164-CUC1/2 module was also suggested to suppress shoot-meristem formation in postembryonic development (Koyama et al. 2007, Koyama et al. 2010). However, as our data show no reduction in *CUC1* and *CUC2* expression in

hen1 explants (Supplementary Figs. S2, S6), this regulatory module does not seem to act as a causal instrument for the impaired de novo shoot regeneration of *hen1*. Recently, Rubio-Somoza et al. (2014) reported that TCPs interfere with CUC activity in an miR164-independent manner feasibly by affecting CUC dimerization and transactivation potential. Therefore, it is possible that the illegitimate posttranslational inhibition of CUC activity by increased levels of TCP3/4 in *hen1* might also contribute to the impaired shoot regeneration. The incompletely rescued shoot-regeneration phenotype of the *hen1-6 tcp4-1* mutants (**Fig. 5B, C**) that have a lower *ARR16* transcript level than WT (**Fig. 6B**) suggests the existence of an additional regulatory module that is independent of the miR319-TCP3/4-ARR16 module. The posttranslational regulation of CUC activity by TCPs might have the potential for such regulation.
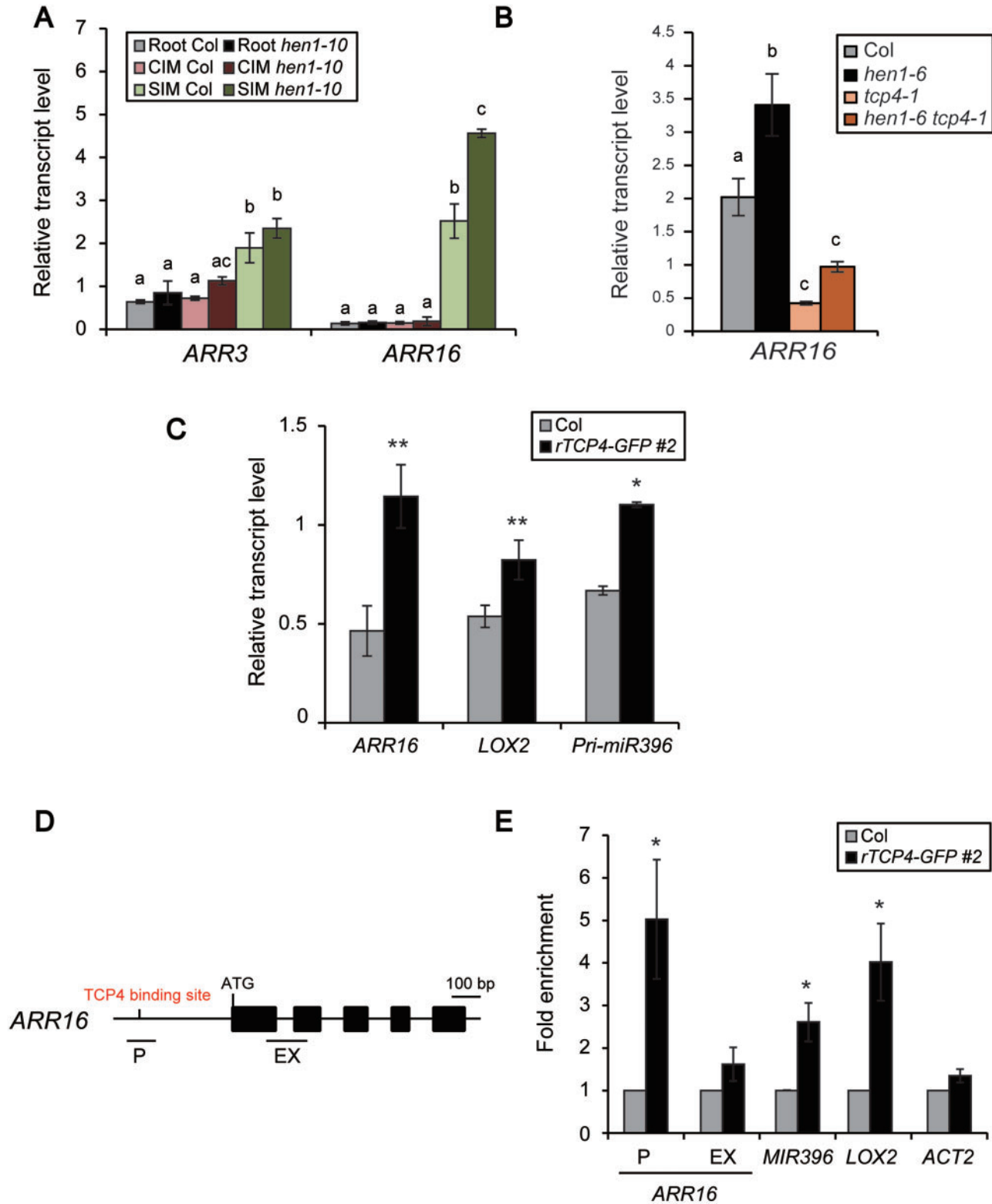
Fig. 6 TCP4 directly upregulates *ARR16* expression during shoot regeneration. (A) RT-qPCR analysis of *ARR3* and *ARR16* transcript levels in Col and *hen-10*. Roots of 2-week-old seedlings, 7-day CIM-incubated root explants and 7-day CIM-incubated + 4-day SIM-incubated root explants were used for RNA extraction. (B) RT-qPCR analysis of *ARR16* transcript levels in Col, *hen1-6*, *tcp4-1* and *hen1-6 tcp4-1* root-derived explants incubated 7 d on CIM + 4 d on SIM. (C) RT-qPCR analysis of the transcript levels of known TCP4-target genes in Col and *rTCP4-GFP* root-derived explants incubated 7 d on CIM + 4 d on SIM. (D) Schematic representation of the *ARR16* loci. Regions (P and EX) tested for ChIP-qPCR analysis in (E) are marked. Black boxes indicate exons, and lines represent intergenic regions or introns. The previously reported TCP4-binding site (Efroni et al. 2013) is marked with red letters. (E) ChIP-qPCR analysis of the targeting activity of rTCP4-GFP protein to the TCP4-binding sites using the anti-GFP antibody. ARR16 EX and *ACT2* regions were included as negative controls. Seven-day CIM-incubated + 4-day SIM-incubated root-derived explants were used for ChIP

Materials and Methods

Plant materials and growth conditions

All the *A. thaliana* mutants and transgenic plants used in this study are in the Columbia-0 (Col-0) background. *hen1-10* was originally isolated as a late-flowering mutant from our screen of flowering phenotypes using a T-DNA insertion population. Later, the mutant phenotype showed independent segregation from the T-DNA, and a single-base-pair deletion in the fifth exon of *HEN1*, which causes an early stop codon at amino acid 641 of the HEN1 protein, was identified through map-based cloning and whole-genome sequencing analysis. *hen1-5* (SALK_049197) and *hen1-6* (SALK_090960) were obtained from TAIR (**http://www.arabidopsis.org**). *35S::rSPL3* (Wu et al. 2009), *pSPL9::rSPL9* (Wang et al. 2009, Kim et al. 2015), *TCS::GFP* (Iwase et al. 2011), *pWUS::mGFP-ER* (Gordon et al. 2007), *tcp4-1* (SAIL_1174; Schommer et al. 2008), *35S::mTCP3*, *tcp3/4/10* and *tcp3/4/5/10/13* (Koyama et al. 2010) were described previously. Individual *tcp* mutant alleles used for the construction of *tcp3/4/10* and *tcp3/4/5/10/13* were *tcp3-1* (CS855978; Koyama et al. 2007), *tcp4-1* (GK_363H08; Rosso et al. 2003), *tcp5-1* (SM_3_29639; Tissier et al. 1999; Efroni et al. 2008), *tcp10-1* (SALK_137205; Alonso et al. 2003) and *tcp13-2* (GK_182B12; Koyama et al. 2010). For *hen1*-containing double mutants, indicated single mutants were crossed with *hen1-10* or *hen1-6* and homozygous double plants were selected in the F2 or F3 populations by genotyping.

Plants were grown under $100\ \mu\text{mol m}^{-2}\,\text{s}^{-1}$ cool white fluorescent lights in long days (16-h light and 8-h dark photoperiod) at 22°C. Seeds were surface sterilized with 75% ethanol containing 0.05% Triton X-100 and germinated on Murashige and Skoog (MS) medium supplemented with 1% sucrose and 0.8% phytoagar and buffered to pH 5.7 with 0.05% MES after 2 d imbibition at 4°C in the dark.

Constructs and plant transformation

pTCP4::rTCP4:GFP (*rTCP4-GFP*) construct was previously described (Schommer et al. 2014). For the overexpression of an miR396-resistant form of *GRF1* (*rGRF1*), we constructed *35S::rGRF1* as described by Hewezi et al. (2012): in brief, the miR396-binding site mutations in *rGRF1* were introduced through three sequential PCR reactions. As the first round of PCR, the 5' region of *GRF1* containing the mutated miR396-binding site was amplified using GRF1-XbaI (F1) and GRF1 (R1) primers (**Supplementary Table S4**). Then, the 3' region of *GRF1* containing the mutated miR396-binding site was amplified using GRF1 (F2) and GRF1-SacI (R2) primers (**Supplementary Table S4**). Finally, we used purified PCR products from the above reactions to amplify the full-length *rGRF1*, which contains the mutated miR396-binding sites using GRF1-XbaI (F1) and GRF1-SacI (R2) primers (**Supplementary Table S4**), and the PCR product was cloned into the binary vector pBI121. *pTCP4::rTCP4:GFP* and *35S::rGRF1* constructs were then transformed into Col-0 plants via *Agrobacterium*-mediated transformation using the floral dip method (Clough and Bent 1998). Homozygous transgenic plants were selected in the subsequent generations through kanamycin-resistance assay on MS medium and genotyping.

Regeneration assay

The culture was based on Gamborg's B5 medium with minimal organics (Sigma-Aldrich) supplemented with 3% sucrose and buffered to pH 5.7 with 0.05% MES and 0.8% phytoagar. A total of 0.5 mg/l of 2,4-dichlorophenoxyacetic acid (2,4-D) and 0.1 mg/l of kinetin were included in CIM. A total of 158 μg/l of IAA and 894 μg/l of 2IP or 158 μg/l of IAA was included in SIM or RIM, respectively. Root explants were collected from 14- to 20-day-old seedlings and incubated first on CIM for indicated periods at 22°C in the dark. Then, for the shoot or root regeneration, the CIM-incubated explants were transferred onto SIM or RIM and incubated further for indicated periods at 22°C under continuous light or in the dark, respectively. Images of explants were observed under a stereomicroscope (Carl Zeiss STEMI 2000-C).

Microscopy

Confocal images were observed with Carl Zeiss LSM700, and GFP signals were visualized by excitation at 488 nm and detection at 495–550 nm. A total of 50 μg/ml of propidium iodide (PI) was used for the staining of the cell outlines. Approximately 20 root explants were observed to infer the representative pattern of each sample.

Histochemical GUS assay

GUS staining was performed as described previously (Han et al. 2007). At least 20 root-derived explants were stained for each genotype and stage to infer the representative pattern. GUS images were observed under a stereomicroscope (Carl Zeiss STEMI 2000-C).

Quantification of anthocyanin content

Seedlings were collected after ±benzyladenine (BA) treatment, ground into fine powder in liquid nitrogen and extracted with 80% methanol containing 1% HCl overnight in the dark at 4°C with shaking. The 1:1 ratio of water and chloroform was then added into each sample and mixed. After centrifugation at $12,000 \times g$ for 2 min, the amounts of anthocyanin were quantified photometrically using the supernatant. Finally, the collected absorbance was calculated by $(A_{530} - 0.25 \times A_{657})$/fresh weight of the seedlings (Rabino and Mancinelli 1986).

RNA isolation and RT-qPCR analysis

Total RNA was isolated using TRI Reagent (MRC), and 1 or 2 μg of it was RT in a 20-μl reaction using reverse transcriptase (Invitrogen) to provide the cDNA template for qPCR analysis. qPCR was performed with the Rotor-Gene Q real-time PCR cycler (Qiagen) using SYBR premix (KAPA or TAKARA). Transcript levels were normalized to the level of the internal control *Ubiquitin 10* (*UBQ10*). For stem-loop RT-qPCR of mature miR319, multiplexed RT (Varkonyi-Gasic and Hellens 2007) was performed using miR319 (RT) and U6 (RT) primers and qPCR was performed with miR319 (F)/Universal reverse primer and U6 (F)/Universal reverse primer, respectively. Mature miR319 transcript level was normalized to U6. The experiments were repeated at least three times for each gene, and the values were presented as the means ± SE of at least three biological replicates. Gene-specific primers used are listed in **Supplementary Table S4**.

RNA-seq analysis

RNA-seq and alignment procedures were conducted by ChunLab (Seoul, South Korea). Libraries for Illumina sequencing were made with TruSeq Stranded mRNA sample preparation kit (Illumina) following the manufacturer's protocol. RNA-seq was performed on the Illumina HiSeq™ 2500 platform to generate paired-end 100-bp reads. The reference-genome sequence was retrieved from the TAIR database (**https://www.arabidopsis.org/**). Quality-filtered reads were aligned to the reference-genome sequence using Bowtie2. The relative transcript abundance was calculated by the reads per kilobase of exon sequence per million mapped sequence reads (RPKM) method. Visualization of mapping results and DEG analysis were performed using the CLRNASeq™ program (ChunLab, South Korea).

ChIP-qPCR assay

ChIP was performed as previously described (Choi et al. 2012) using calli incubated 4 d on SIM after a 1-week preincubation on CIM. Briefly, 0.2 g of calli were vacuum infiltrated with 1% formaldehyde for cross-linking and ground in liquid nitrogen after quenching the cross-linking process. Chromatin was isolated and sonicated into approximately 0.5–1 kb fragments. Chromatin solution was precleared for 1 h with 40 μl of salmon sperm DNA/Protein A agarose beads (Millipore 16–157). Then, 5 μl of GFP antibody (Roche 11814460001) was added and incubated for overnight at 4°C. After subsequent incubation with 4 μl of salmon sperm DNA/Protein A agarose beads, immune complexes were precipitated and eluted from the beads. Cross-links were reversed, and residual proteins in the immune

Fig. 6 Continued

assay. Col levels were set to 1 after normalization to corresponding input DNAs. Shown are the means ± SE of three biological replicates after normalization with the internal control *UBQ10* (A–C) or input DNA (E). The asterisks indicate statistically significant differences compared to Col levels (*$P < 0.01$ and **$P < 0.005$ in Student's *t*-test) (C and E). Different letters indicate statistically significant different groups ($P < 0.05$) by one-way ANOVA with Tukey's post hoc test (A and B).

Fig. 7 The *hen1-6* mutation results in an altered spatial expression pattern and downregulation of *WUS* in SIM-incubated explants. (A) *pWUS::mGFP5-ER* expression in Col and *hen1-6* root-derived explants preincubated 14 d on CIM and then transferred onto and further incubated on SIM for indicated days. Cellular outlines were visualized with PI staining (red). Scale bars: 50 μm. Greater than or equal to 10 independent explants of each genotype and time point were observed and representative images are shown. (B) RT-qPCR analysis of *WUS* transcript levels in Col and *hen1-6* root-derived explants incubated 14 d on CIM + 12 d on SIM. Shown are the means ± SE of three biological replicates. The Col level was set to 1 after normalization with *UBQ10* ($^*P < 0.01$ in Student's *t*-test).

complexes were removed by incubating with proteinase K (Roche 03115828001) followed by DNA purification using the QIAquick PCR Purification Kit (Qiagen 28106). The relative amount of chromatin immunoprecipitated DNA was determined by qPCR following the $\Delta\Delta C_T$ method and normalization of the respective input DNA. The fold enrichments were calculated by comparing to non-transgenic WT values, which were set to 1 after normalization to the levels of input DNA. The values were presented as the means ± SE of three biological replicates. Primers used for ChIP-qPCR are listed in **Supplementary Table S4**.

Statistical analysis

Significant differences between the two samples were determined by Student's *t*-tests. One-way ANOVA followed by Tukey's post hoc tests was used for multiple samples to evaluate significant differences ($P < 0.05$) as described in the figure legends.

Supplementary Data

Supplementary data are available at PCP online.

Disclosures

The authors have no conflict of interest to declare.

References

Alonso, J.M., Stepanova, A.N., Leisse, T.J., Kim, T.J., Chen, H., Shinn, P., et al. (2003) Genome-wide insertional mutagenesis of *Arabidopsis thaliana*. *Science* 301: 653–657.

Alvarez, J.P., Furumizu, C., Efroni, I., Eshed, Y. and Bowman, J.L. (2016) Active suppression of a leaf meristem orchestrates determinate leaf growth. *Elife* 5: e15023.

Atta, R., Laurens, L., Boucheron-Dubuisson, E., Guivarc'h, A., Carnero, E., Giraudat-Pautot, V., et al. (2009) Pluripotency of Arabidopsis xylem pericycle underlies shoot regeneration from root and hypocotyl explants grown in vitro. *Plant J.* 57: 626–644.

Bülow, L., Bolívar, J.C., Ruhe, J., Brill, Y. and Hehl, R. (2012) 'MicroRNA Targets', a new AthaMap web-tool for genome-wide identification of miRNA targets in *Arabidopsis thaliana*. *BioData Mining* 5: 7.

Buechel, S., Leibfried, A., To, J.P., Zhao, Z., Andersen, S.U., Kieber, J.J., et al. (2010) Role of A-type ARABIDOPSIS RESPONSE REGULATORS in meristem maintenance and regeneration. *Eur. J. Cell Biol.* 89: 279–284.

Cary, A.J., Che, P. and Howell, S.H. (2002) Developmental events and shoot apical meristem gene expression patterns during shoot development in *Arabidopsis thaliana*. *Plant J.* 32: 867–877.

Chatfield, S.P., Capron, R., Severino, A., Penttila, P.A., Alfred, S., Nahal, H., et al. (2013) Incipient stem cell niche conversion in tissue culture: using a systems approach to probe early events in WUSCHEL-dependent conversion of lateral root primordia into shoot meristems. *Plant J.* 73: 798–813.

Choi, S.M., Song, H.R., Han, S.K., Han, M., Kim, C.Y., Park, J., et al. (2012) HDA19 is required for the repression of salicylic acid biosynthesis and salicylic acid-mediated defense responses in Arabidopsis. *Plant J.* 71: 135–146.

Clough, S.J. and Bent, A.F. (1998) Floral dip: a simplified method for Agrobacterium-mediated transformation of *Arabidopsis thaliana*. *Plant J.* 16: 735–743.

Earley, K., Smith, M., Weber, R., Gregory, B. and Poethig, R. (2010) An endogenous F-box protein regulates ARGONAUTE1 in *Arabidopsis thaliana*. *Silence* 1: 15.

Efroni, I., Blum, E., Goldshmidt, A. and Eshed, Y. (2008) A protracted and dynamic maturation schedule underlies Arabidopsis leaf development. *Plant Cell* 20: 2293–2306.

Efroni, I., Han, S.K., Kim, H.J., Wu, M.F., Steiner, E., Birnbaum, K.D., et al. (2013) Regulation of leaf maturation by chromatin-mediated modulation of cytokinin responses. *Dev. Cell* 24: 438–445.

Gonzalez, N., De Bodt, S., Sulpice, R., Jikumaru, Y., Chae, E., Dhondt, S., et al. (2010) Increased leaf size: different means to an end. *Plant Physiol.* 153: 1261–1279.

Gordon, S.P., Heisler, M.G., Reddy, G.V., Ohno, C., Das, P. and Meyerowitz, E.M. (2007) Pattern formation during de novo assembly of the Arabidopsis shoot meristem. *Development* 134: 3539–3548.

Han, S.K., Song, J.D., Noh, Y.S. and Noh, B. (2007) Role of plant CBP/p300-like genes in the regulation of flowering time. *Plant J.* 49: 103–114.

Hewezi, T., Maier, T.R., Nettleton, D. and Baum, T.J. (2012) The Arabidopsis microRNA396-GRF1/GRF3 regulatory module acts as a developmental regulator in the reprogramming of root cells during cyst nematode infection. *Plant Physiol.* 159: 321–335.

Horiguchi, G., Kim, G.T. and Tsukaya, H. (2005) The transcription factor AtGRF5 and the transcription coactivator AN3 regulate cell proliferation in leaf primordia of *Arabidopsis thaliana*. *Plant J.* 43: 68–78.

Iwase, A., Mitsuda, N., Koyama, T., Hiratsu, K., Kojima, M., Arai, T., et al. (2011) The AP2/ERF transcription factor WIND1 controls cell dedifferentiation in Arabidopsis. *Curr. Biol.* 21: 508–514.

Kareem, A., Durgaprasad, K., Sugimoto, K., Du, Y., Pulianmackal, A.J., Trivedi, Z.B., et al. (2015) *PLETHORA* genes control regeneration by a two-step mechanism. *Curr. Biol.* 25: 1017–1030.

Kim, J.H. and Kende, H. (2004) A transcriptional coactivator, AtGIF1, is involved in regulating leaf growth and morphology in Arabidopsis. *Proc. Natl. Acad. Sci. USA* 101: 13374–13379.

Kim, J.Y., Oh, J.E., Noh, Y.S. and Noh, B. (2015) Epigenetic control of juvenile-to-adult phase transition by the Arabidopsis SAGA-like complex. *Plant J.* 83: 537–545.

Kim, J.Y., Yang, W., Forner, J., Lohmann, J.U., Noh, B. and Noh, Y.S. (2018) Epigenetic reprogramming by histone acetyltransferase HAG1/AtGCN5 is required for pluripotency acquisition in Arabidopsis. *EMBO J.* 37: e98726.

Koyama, T., Furutani, M., Tasaka, M. and Ohme-Takagi, M. (2007) TCP transcription factors control the morphology of shoot lateral organs via negative regulation of the expression of boundary-specific genes in Arabidopsis. *Plant Cell* 19: 473–484.

Koyama, T., Mitsuda, N., Seki, M., Shinozaki, K. and Ohme-Takagi, M. (2010) TCP transcription factors regulate the activities of ASYMMETRIC LEAVES1 and miR164, as well as the auxin response, during differentiation of leaves in Arabidopsis. *Plant Cell* 22: 3574–3588.

Koyama, T., Sato, F. and Ohme-Takagi, M. (2017) Roles of miR319 and TCP transcription factors in leaf development. *Plant Physiol.* 175: 874–885.

Laplaze, L., Benkova, E., Casimiro, I., Maes, L., Vanneste, S., Swarup, R., et al. (2007) Cytokinins act directly on lateral root founder cells to inhibit root initiation. *Plant Cell* 19: 3889–3900.

Li, C. and Zhang, B. (2016) MicroRNAs in control of plant development. *J. Cell. Physiol.* 231: 303–313.

Liu, D., Song, Y., Chen, Z. and Yu, D. (2009) Ectopic expression of miR396 suppresses GRF target gene expression and alters leaf growth in Arabidopsis. *Physiol. Plant.* 136: 223–236.

Liu, Z., Li, J., Wang, L., Li, Q., Lu, Q., Yu, Y., et al. (2016) Repression of callus initiation by the miRNA-directed interaction of auxin-cytokinin in *Arabidopsis thaliana*. *Plant J.* 87: 391–402.

Meng, W.J., Cheng, Z.J., Sang, Y.L., Zhang, M.M., Rong, X.F., Wang, Z.W., et al. (2017) Type-B ARABIDOPSIS RESPONSE REGULATORs specify the shoot stem cell niche by dual regulation of WUSCHEL. *Plant Cell* 29: 1357–1372.

Palatnik, J.F., Allen, E., Wu, X., Schommer, C., Schwab, R., Carrington, J.C., et al. (2003) Control of leaf morphogenesis by microRNAs. *Nature* 425: 257–263.

Park, W., Li, J., Song, R., Messing, J. and Chen, X. (2002) CARPEL FACTORY, a Dicer homolog, and HEN1, a novel protein, act in microRNA metabolism in *Arabidopsis thaliana*. *Curr. Biol.* 12: 1484–1495.

Qiao, M. and Xiang, F. (2013) A set of *Arabidopsis thaliana* miRNAs involve shoot regeneration in vitro. *Plant Signal. Behav.* 8: e23479.

Qiao, M., Zhao, Z., Song, Y., Liu, Z., Cao, L., Yu, Y., et al. (2012) Proper regeneration from in vitro cultured *Arabidopsis thaliana* requires the microRNA-directed action of an auxin response factor. *Plant J.* 71: 14–22.

Rabino, I. and Mancinelli, A.L. (1986) Light, temperature, and anthocyanin production. *Plant Physiol.* 81: 922–924.

Ren, B., Liang, Y., Deng, Y., Chen, Q., Zhang, J., Yang, X., et al. (2009) Genome-wide comparative analysis of type-A Arabidopsis response regulator genes by overexpression studies reveals their diverse roles and regulatory mechanisms in cytokinin signaling. *Cell Res.* 19: 1178–1190.

Ren, G., Xie, M., Zhang, S., Vinovskis, C., Chen, X. and Yu, B. (2014) Methylation protects microRNAs from an AGO1-associated activity that uridylates 5′ RNA fragments generated by AGO1 cleavage. *Proc. Natl. Acad. Sci. USA* 111: 6365–6370.

Rodriguez, R.E., Mecchia, M.A., Debernardi, J.M., Schommer, C., Weigel, D. and Palatnik, J.F. (2010) Control of cell proliferation in *Arabidopsis thaliana* by microRNA miR396. *Development* 137: 103–112.

Rosso, M.G., Li, Y., Strizhov, N., Reiss, B., Dekker, K. and Weisshaar, B. (2003) An Arabidopsis *thaliana* T-DNA mutagenized population (GABI-Kat) for flanking sequence tag-based reverse genetics. *Plant Mol. Biol.* 53: 247–259.

Rubio-Somoza, I., Zhou, C.-M., Confraria, A., Martinho, C., Von born, P., Baena-Gonzalez, E., et al. (2014) Temporal Control of Leaf Complexity by miRNA-Regulated Licensing of Protein Complexes. *Curr. Biol.* 24: 2714–2719.10.1016/j.cub.2014.09.058

Schommer, C., Debernardi, J.M., Bresso, E.G., Rodriguez, R.E. and Palatnik, J.F. (2014) Repression of cell proliferation by miR319-regulated TCP4. *Mol. Plant* 7: 1533–1544.

Schommer, C., Palatnik, J.F., Aggarwal, P., Chetelat, A., Cubas, P., Farmer, E.E., et al. (2008) Control of jasmonate biosynthesis and senescence by miR319 targets. *PLoS Biol.* 6: e230.

Skoog, F. and Miller, C.O. (1957) Chemical regulation of growth and organ formation in plant tissues cultured in vitro. *Symp. Soc. Exp. Biol.* 11: 118–130.

Sugimoto, K., Gordon, S.P. and Meyerowitz, E.M. (2011) Regeneration in plants and animals: dedifferentiation, transdifferentiation, or just differentiation? *Trends Cell Biol.* 21: 212–218.

Sugimoto, K., Jiao, Y. and Meyerowitz, E.M. (2010) Arabidopsis regeneration from multiple tissues occurs via a root development pathway. *Dev. Cell* 18: 463–471.

Sunkar, R., Li, Y.F. and Jagadeeswaran, G. (2012) Functions of microRNAs in plant stress responses. *Trends Plant Sci.* 17: 196–203.

Tang, X., Bian, S., Tang, M., Lu, Q., Li, S., Liu, X., et al. (2012) MicroRNA-mediated repression of the seed maturation program during vegetative development in Arabidopsis. *PLoS Genet.* 8: e1003091.

Tissier, A.F., Marillonnet, S., Klimyuk, V., Patel, K., Torres, M.A., Murphy, G., et al. (1999) Multiple independent defective suppressor-mutator transposon insertions in Arabidopsis: a tool for functional genomics. *Plant Cell* 11: 1841–1852.

Tsai, H.L., Li, Y.H., Hsieh, H.P., Lin, M.C., Ahn, J.H. and Wu, S.H. (2014) HUA ENHANCER1 is involved in posttranscriptional regulation of positive and negative regulators in Arabidopsis photomorphogenesis. *Plant Cell* 26: 2858–2872.

Varkonyi-Gasic, E. and Hellens, R.P. (2007) Quantitative stem-loop RT-PCR for detection of microRNAs. *Methods Mol. Biol.* 744: 145–157.

Vazquez, F., Gasciolli, V., Crété, P. and Vaucheret, H. (2004) The nuclear dsRNA binding protein HYL1 is required for microRNA accumulation and plant development, but not posttranscriptional transgene silencing. *Curr. Biol.* 14: 346–351.

Wang, J., Tian, C., Zhang, C., Shi, B., Cao, X., Zhang, T.Q., et al. (2017) Cytokinin signaling activates WUSCHEL expression during axillary meristem initiation. *Plant Cell* 29: 1373–1387.

Wang, J.W., Czech, B. and Weigel, D. (2009) MiR156-regulated SPL transcription factors define an endogenous flowering pathway in *Arabidopsis thaliana*. *Cell* 138: 738–749.

Wang, X., Wang, Y., Dou, Y., Chen, L., Wang, J., Jiang, N., et al. (2018) Degradation of unmethylated miRNA/miRNA*s by a DEDDy-type 3′ to 5′ exoribonuclease Atrimmer 2 in Arabidopsis. *Proc. Natl. Acad. Sci. USA* 115: E6659–E6667.

Wu, G., Park, M.Y., Conway, S.R., Wang, J.W., Weigel, D. and Poethig, R.S. (2009) The sequential action of miR156 and miR172 regulates developmental timing in Arabidopsis. *Cell* 138: 750–759.

Xie, M., Chen, H., Huang, L., O'Neil, R.C., Shokhirev, M.N. and Ecker, J.R. (2018) A B-ARR-mediated cytokinin transcriptional network directs hormone cross-regulation and shoot development. *Nat. Commun.* 9: 1604.

Xue, T., Dai, X., Wang, R., Wang, J., Liu, Z. and Xiang, F. (2017) ARGONAUTE10 inhibits in vitro shoot regeneration via repression of miR165/166 in *Arabidopsis thaliana*. *Plant Cell Physiol.* 58: 1789–1800.

Zhao, Y., Yu, Y., Zhai, J., Ramachandran, V., Dinh, T.T., Meyers, B.C., et al. (2012) The Arabidopsis nucleotidyl transferase HESO1 uridylates unmethylated small RNAs to trigger their degradation. *Curr. Biol.* 22: 689–694.

Zhang, T.-Q., Lian, H., Tang, H., Dolezal, K., Zhou, C.-M., Yu, S., et al. (2015) An intrinsic microRNA timer regulates progressive decline in shoot regenerative capacity in plants. *Plant Cell* 27: 349–360.

Zhang, T.Q., Lian, H., Zhou, C.M., Xu, L., Jiao, Y. and Wang, J.W. (2017) A two-step model for de novo activation of WUSCHEL during plant shoot regeneration. *Plant Cell* 29: 1073–1087.

Zubo, Y.O., Blakley, I.C., Yamburenko, M.V., Worthen, J.M., Street, I.H., Franco-Zorrilla, J.M., et al. (2017) Cytokinin induces genome-wide binding of the type-B response regulator ARR10 to regulate growth and development in Arabidopsis. *Proc. Natl. Acad. Sci. USA* 114: E5995–E6004.